

Supplementary information

Slow magnetic relaxation in Ni-Ln (*Ln* = Ce, Gd, Dy) dinuclear complexes

Anna Vráblová, Milagros Tomás, Larry R. Falvello, Ľubor Dlháň, Ján Titiš, Juraj Černák, Roman Boča

Analytical data

H₂(o-van-en)

Anal. [%], calculated for C₁₈H₂₀O₄N₂: C, 65.83; H, 6.15; N, 8.53; found: C, 66.30; H, 6.33; N, 8.57. IR (cm⁻¹) of H₂(o-van-en): 3746w, 2997w, 2931w, 2848w, 1631s, 1463s, 1438m, 1408m, 1325w, 1295w, 1246vs, 1189m, 1170m, 1133m, 1080s, 1054m, 1010m, 987m, 962s, 836s, 791s, 782s, 740s, 729s, 620m, 521m, 441m. UV-Vis (nm) in EtOH: 219, 264; in CHCl₃: 265, 334. ¹H-NMR: 3.92 m, 6.84 m, 7.267 s, 8.323 s, 13.5 s, b. ¹³C-NMR: 56.056, 59.467, 114.084, 118.032, 118.419, 123.149, 148.269, 151.402, 166.643.

[Ni(o-van-en)Ce(H₂O)Cl₃] (1)

Yield: 81 %. Anal. [%], calculated for CeNiC₁₈H₂₀Cl₃O₅N₂: C, 33.28; H, 3.10; N, 4.31; found: C, 32.50; H, 3.39; N, 4.30. IR (cm⁻¹) of **1**: 3334wm, 3248m, 2952w, 2926w, 1638m, 1622s, 1608s, 1560m, 1459s, 1431m, 1410w, 1390w, 1342w, 1324w, 1291s, 1243s, 1230s, 1198m, 1165m, 1139w, 1101w, 1077s, 1053m, 989m, 980m, 956s, 900m, 864m, 847m, 783s, 739vs, 686m, 667w, 626m, 579m, 549m, 536m, 494m, 440s, 408s. Single crystals suitable for X-ray analysis were obtained by recrystallization of the microcrystalline complex using room temperature diffusion of a MeOH solution into iPrOH.

[Ni(o-van-en)Gd(H₂O)Cl₃] (2)

Yield: 65 %. Anal. [%], calculated for GdNiC₁₈H₂₀Cl₃O₅N₂: C, 32.43; H, 3.02; N, 4.20; found: C, 31.82; H, 2.73; N, 4.23. IR (cm⁻¹) of **2**: 3347wm, 3242m, 2949w, 2927w, 1622s, 1609s, 1560m, 1471s, 1462s, 1435m, 1409m, 1390w, 1340w, 1323w, 1295s, 1247s, 1230s, 1198m, 1166m, 1142w, 1100w, 1077s, 1053m, 988m, 980m, 957s, 902m, 866m, 845m, 783s, 739vs, 692m, 669w, 629m, 580m, 550m, 539m, 497m, 442m, 409s. Single crystals of [Ni(o-van-en)Gd(H₂O)Cl₃] (**2**) were obtained by crystallization using diffusion of a MeOH solution of GdCl₃ into an iPrOH solution of [Ni(o-van-en)] at room temperature.

[Ni(o-van-en)Dy(H₂O)Cl₃] (3)

Yield: 70 %. Anal. [%], calculated for DyNiC₁₈H₂₀Cl₃O₅N₂: C, 32.18; H, 3.00; N, 4.17; found: C, 31.36; H, 3.23; N, 4.00. IR (cm⁻¹) of **3**: 3342wm, 3242m, 2949w, 2928w, 1623s, 1610s, 1560m, 1462s, 1436m, 1400m, 1389w, 1340w, 1323w, 1294s, 1248s, 1229s, 1197m, 1166m, 1077s, 1053m, 988m, 978m, 958s, 903w, 866m, 788s, 739vs, 693m, 669w, 630m, 580m, 550m, 497m, 443m, 409s. Crystals of [Ni(o-van-en)Dy(H₂O)Cl₃] (**3**) were obtained by recrystallization using diffusion of a methanol solution of the microcrystalline product into iPrOH with a temperature gradient of from 70 °C at the bottom of the beaker to room temperature at the top of the solution.

Structural data

Table S1. Crystal data and structure refinement for **1**, **2** and **3**.

	1	2	3
Empirical formula	C ₁₈ H ₂₀ Cl ₃ CeN ₂ NiO ₅	C ₁₈ H ₂₀ Cl ₃ GdN ₂ NiO ₅	C ₁₈ H ₂₀ Cl ₃ DyN ₂ NiO ₅
Formula weight [g.mol ⁻¹]	649.54	666.67	671.92
Crystal system, space group	monoclinic, <i>P</i> 2 ₁ / <i>n</i>	monoclinic, <i>P</i> 2 ₁ / <i>n</i>	monoclinic, <i>P</i> 2 ₁ / <i>n</i>
Unit cell dimensions and unit cell volume [Å, °, Å ³]	<i>a</i> = 7.1269(3) <i>b</i> = 14.4698(6) <i>c</i> = 21.0732(12) β = 93.014(4) <i>V</i> = 2170.18(18)	<i>a</i> = 7.0236(3) <i>b</i> = 14.3753(9) <i>c</i> = 20.9662(13) β = 92.216(5) <i>V</i> = 2115.3(2)	<i>a</i> = 7.00940(10) <i>b</i> = 14.3916(3) <i>c</i> = 20.9556(5) β = 91.833(2) <i>V</i> = 2112.85(7)
<i>Z</i>	4	4	4
Calculated density [g cm ⁻³]	1.988	2.093	2.112
Absorption coefficient [mm ⁻¹]	3.341	4.411	4.813
Crystal form, colour, size [mm]	dichroic red-orange and colourless blocks, 0.091 x 0.057 x 0.018	pale orange block, 0.175 x 0.079 x 0.034	red/colourless dichroic, rhombic, 0.08 x 0.04 x 0.02
Temperature [K]	299(2)	295(2)	293(2)
Radiation [Å]	Mo <i>K</i> _α (λ = 0.71073)	Mo <i>K</i> _α (λ = 0.71073)	Mo <i>K</i> _α (λ = 0.71073)
Diffractometer	XCalibur, CCD detector	XCalibur, CCD detector	XCalibur, CCD detector
θ range for data collection [°]	3.653 - 28.384	3.230 - 24.997	2.831 - 30.302
Index ranges	-9 ≤ <i>h</i> ≤ 9, -19 ≤ <i>k</i> ≤ 19, -28 ≤ <i>l</i> ≤ 26	-8 ≤ <i>h</i> ≤ 8, -10 ≤ <i>k</i> ≤ 17, -24 ≤ <i>l</i> ≤ 23	-9 ≤ <i>h</i> ≤ 8, -20 ≤ <i>k</i> ≤ 19, -29 ≤ <i>l</i> ≤ 28
Reflections collected / independent	6159 / 6159	9912 / 3716	26349 / 5820
GooF (<i>S</i>)	0.972	0.943	1.038
Final <i>R</i> indices [<i>I</i> > 2σ(<i>I</i>)]	<i>R</i> 1 = 0.0370, w <i>R</i> 2 = 0.0990	<i>R</i> 1 = 0.0589, w <i>R</i> 2 = 0.0692	<i>R</i> 1 = 0.0338, w <i>R</i> 2 = 0.0587
Final <i>R</i> indices (all data)	<i>R</i> 1 = 0.0642, w <i>R</i> 2 = 0.1051	<i>R</i> 1 = 0.1320, w <i>R</i> 2 = 0.0864	<i>R</i> 1 = 0.0671, w <i>R</i> 2 = 0.0587
Largest diff. peak and hole [e.Å ⁻³]	-0.640 ≤ Δρ ≤ 0.708	-1.148 ≤ Δρ ≤ 1.613	-0.821 ≤ Δρ ≤ 0.677

Table S2. Potential hydrogen bonds in **1**, **2** and **3**.

D-H···A	D-H [Å]	H···A [Å]	D···A [Å]	D-H···A [°]
1				
O5-H1W···Cl3 ⁱ	0.845(11)	2.32(3)	3.122(5)	157(7)
O5-H2W···Cl2 ⁱ	0.842(11)	2.35(3)	3.125(5)	154(6)
C11-H11···Cl2 ⁱⁱ	0.93	2.65	3.577(8)	178.9
2				
O5-H1W···Cl3 ⁱ	0.85	2.36	3.146(7)	155.0
O5-H2W···Cl2 ⁱ	0.88	2.34	3.147(8)	152.8
C11-H11···Cl2 ⁱⁱ	0.95(10)	2.63(10)	3.572(13)	173(9)
3				
O5-H1W···Cl3 ⁱ	0.836(10)	2.363(18)	3.149(3)	157(3)
O5-H2W···Cl2 ⁱ	0.836(10)	2.39(2)	3.148(3)	151(3)
C11-H11···Cl2 ⁱⁱ	0.93	2.63	3.562(4)	176.9

Symmetry codes: i: 1 + x, y, z; ii: -1/2 - x, 1/2 + y, 1/2 - z.

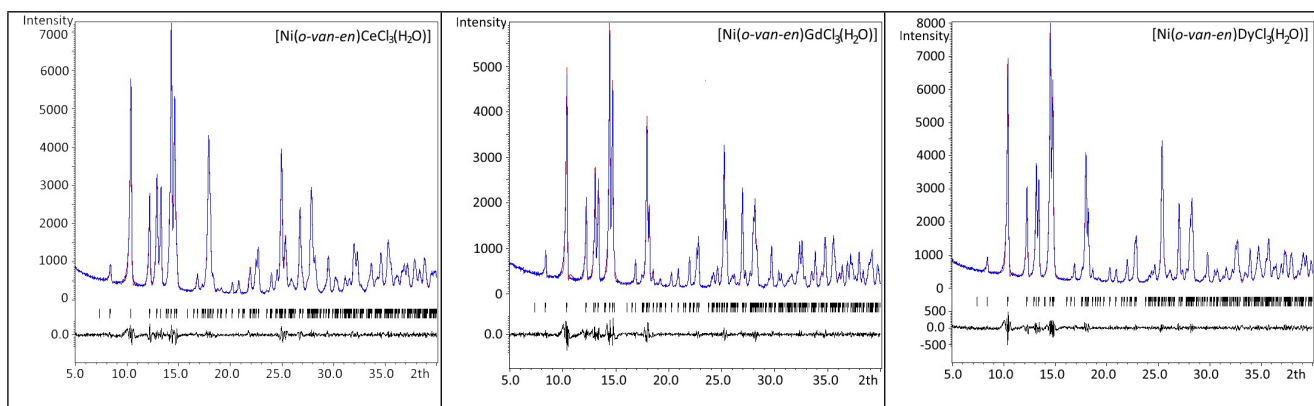


Figure S1. LeBail refinement of the measured powder diffraction patterns of complexes **1**, **2** and **3**, respectively. Red line represents the refined pattern; blue line represents measured data; black line represents the difference. Herewith, we give the input and refined unit cell parameters [in brackets] and values of $R(p)$, $R(wp)$ and Goof for samples **1**, **2** and **3**, respectively: (**1**) input unit cell parameters [$a = 7.1269$ (3) Å, $b = 14.4698$ (6) Å, $c = 21.0732$ (12) Å, $\alpha = 90^\circ$, $\beta = 93.014$ (4)°, $\gamma = 90^\circ$], refined unit cell [$a = 7.119$ (13) Å, $b = 14.46$ (3) Å, $c = 21.02$ (4) Å, $\alpha = 90^\circ$, $\beta = 92.741$ (6)°, $\gamma = 90^\circ$], $R(p) = 0.0396$, $R(wp) = 0.0544$, Goof = 1.52; (**2**) input unit cell parameters [$a = 7.0236$ (3) Å, $b = 14.3753$ (9) Å, $c = 20.9662$ (13) Å, $\alpha = 90^\circ$, $\beta = 92.216$ (5)°, $\gamma = 90^\circ$], refined unit cell [$a = 7.023$ (3) Å, $b = 14.381$ (6) Å, $c = 20.901$ (9) Å, $\alpha = 90^\circ$, $\beta = 92.173$ (6)°, $\gamma = 90^\circ$], $R(p) = 0.0490$, $R(wp) = 0.0690$, Goof = 1.65; (**3**) input unit cell parameters [$a = 7.00940$ (10) Å, $b = 14.3916$ (3) Å, $c = 20.9556$ (5) Å, $\alpha = 90^\circ$, $\beta = 91.833$ (2)°, $\gamma = 90^\circ$], refined unit cell [$a = 7.0128$ (9) Å, $b = 14.4023$ (19) Å, $c = 20.985$ (3) Å, $\alpha = 90^\circ$, $\beta = 91.803$ (4)°, $\gamma = 90^\circ$], $R(p) = 0.0457$, $R(wp) = 0.0616$, Goof = 1.69.

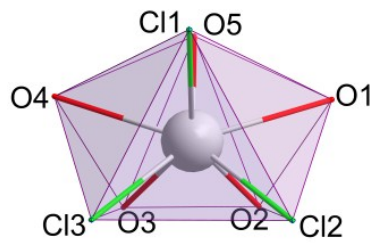


Figure S2. The polyhedron of the Ce(III) central atom in **1**.

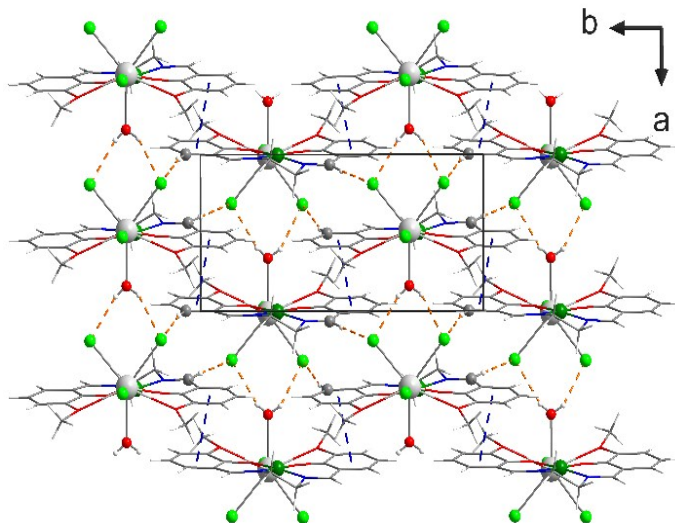


Figure S3. Crystal structure of $[\text{Ni}(\text{o-van-en})\text{Ce}(\text{H}_2\text{O})\text{Cl}_3]$, ab plane. Orange dashed lines represent hydrogen bonds listed in Tab. S2. Blue dashed lines represent π - π stacking interaction between Cg1 of the aromatic ring formed by C2-C7 atoms and Cg2 of the ring formed by C12-C17 atoms with the Cg1…Cg2 distance of 3.619(5) Å [3.630(7) and 3.665(2) Å for **2** and **3**, respectively].

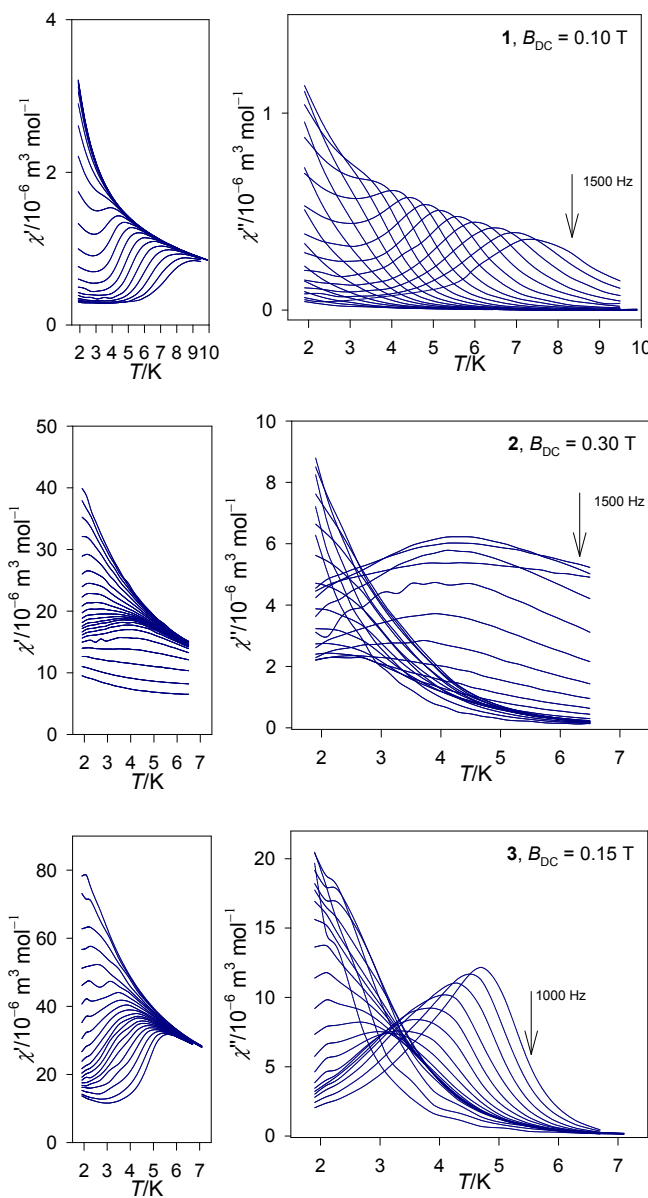


Figure S4. Temperature evolution of the AC susceptibility components for **1**, **2**, and **3**.

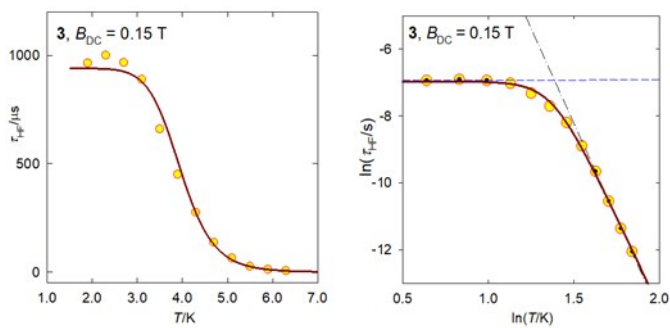


Figure S5. Various representations of the temperature evolution of the HF relaxation time for **3**. Solid curve – fitted with the Raman & tunneling process. Dashed – linear fits for the truncated data.

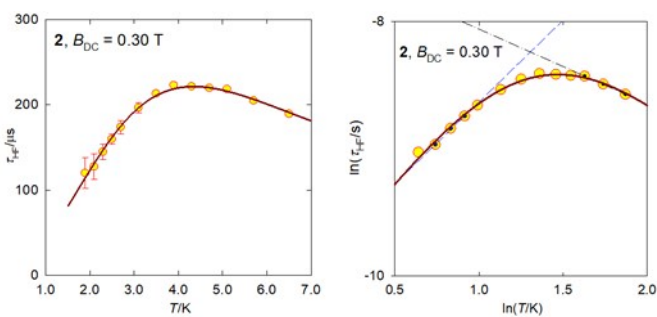


Table S3. Results of the fitting procedure for AC susceptibility components of **1**.

T/K	$R(\chi')$ /%	$R(\chi'')$ /%	χ_S	χ_{LF}	α_{LF}	τ_{LF} /10 ⁻³ s	χ_{HF}	α_{HF}	τ_{HF} /10 ⁻³ s	x_{LF}	x_{HF}
a) $B_{DC} = 0.1$ T											
1.9	0.70	2.3	0.23(1)	2.6(4)	0.06(2)	18.7(11)	3.22(1)	0.26(10)	3.2(28)	0.82	0.18
2.3	1.0	1.7	0.26(2)	2.1(5)	0.05(5)	17.7(15)	2.69(1)	0.25(9)	3.7(27)	0.75	0.25
2.7	0.47	1.6	0.27(1)	1.6(3)	0.01(3)	16.7(10)	2.34(1)	0.21(3)	4.6(18)	0.63	0.37
3.1	0.45	0.15	0.26(1)	1.4(2)	0.01(3)	12.2(5)	2.07(1)	0.27(2)	4.4(13)	0.63	0.37
3.5	0.37	1.2	0.25(1)	1.39(14)	0.02(2)	8.78(26)	1.87(1)	0.27(2)	2.74(88)	0.71	0.29
3.9	0.52	2.4	0.24(2)	1.41(13)	0.02(2)	5.31(15)	1.72(1)	0.39(10)	1.9(12)	0.79	0.21
4.3	0.49	3.1	0.22(6)	1.35(7)	0.01(2)	3.24(7)	1.59(1)	0.50(21)	0.79(141)	0.83	0.17
4.3	1.4	5.2	0.27(1)	1.59(1)	0.09(1)	2.93(5)					
4.7	1.1	4.4	0.27(1)	1.47(1)	0.09(1)	1.93(3)					
5.1	1.0	4.3	0.27(1)	1.39(1)	0.08(1)	1.24(2)					
5.9	1.4	6.2	0.27(1)	1.25(1)	0.08(1)	0.48(1)					
6.7	1.4	7.4	0.24(3)	1.14(1)	0.09(2)	0.195(9)					
7.5	0.87	5.4	0.24(3)	1.05(1)	0.08(2)	0.100(6)					
b) $B_{DC} = 0.5$ T											
1.9	0.82	2.1	0.24(1)	3.01(1)	0.23(1)	60.3(5)				1	
2.3	0.86	2.6	0.23(1)	2.60(1)	0.21(1)	45.0(4)				1	
2.7	1.3	2.4	0.23(1)	2.27(1)	0.18(1)	32.8(4)				1	
3.1	1.4	3.3	0.23(1)	2.01(1)	0.17(1)	22.5(3)				1	
3.5	0.48	1.3	0.21(1)	1.4(2)	0.03(3)	14.4(2)	1.82(1)	0.42(12)	13.5(14)	0.74	0.26
3.9	0.38	0.66	0.21	1.35(10)	0.01(1)	8.50(8)	1.67(1)	0.50(10)	6.8(6)	0.78	0.22

$x_{LF} = (\chi_{T,LF} - \chi_S)/(\chi_T - \chi_S)$, $x_{HF} = (\chi_{T,HF} - \chi_{T,LF})/(\chi_T - \chi_S)$, $\chi_{T,HF} = \chi_T$, and $x_{HF} = 1 - x_{LF}$; χ_i in units of $10^{-6} \text{ m}^3 \text{ mol}^{-1}$.

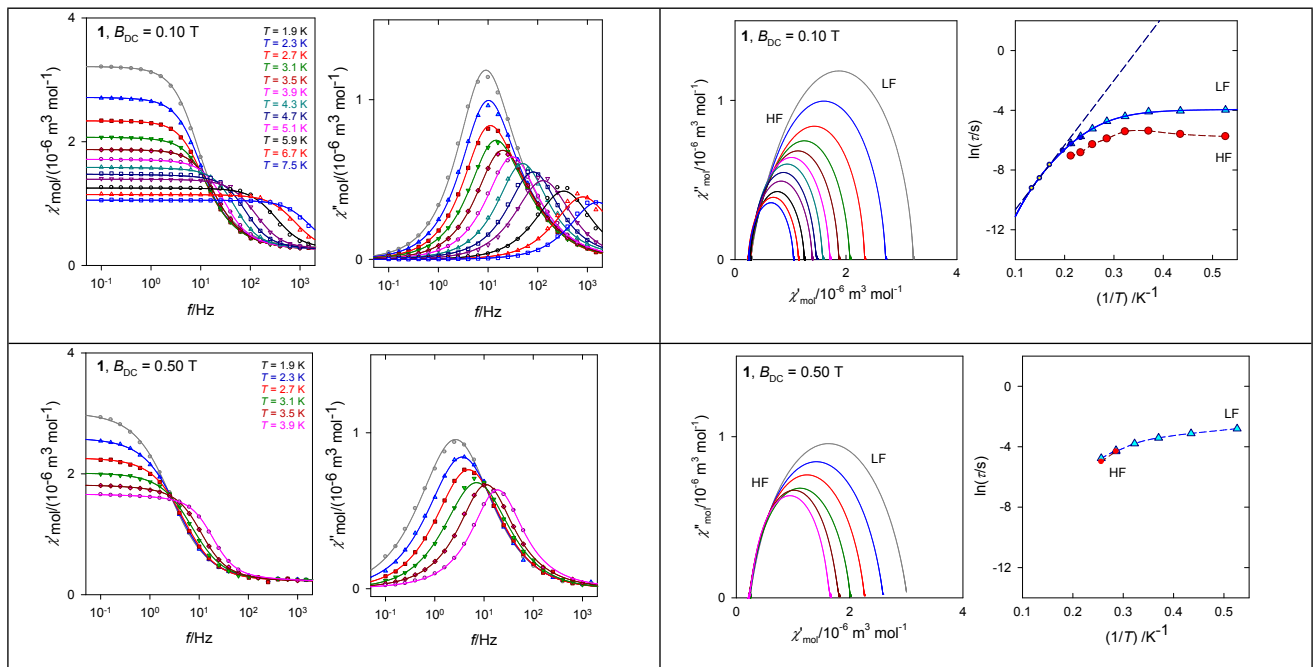
**Figure S7.** AC magnetic data for **1**. Solid lines – fitted by the extended two-set Debye model.

Table S4. Results of the fitting procedure for AC susceptibility components of **2**.

T/K	$R(\chi')$ /%	$R(\chi'')$ /%	χ_S	χ_{LF}	α_{LF}	τ_{LF} $/10^{-3}\text{ s}$	χ_{HF}	α_{HF}	τ_{HF} $/10^{-6}\text{ s}$	x_{LF}	x_{HF}
b) $B_{DC} = 0.3\text{ T}$											
1.9	0.91	3.3	3.3(10)	33(1)	.36(1)	369(13)	46.5(5)	.26(4)	120(18)	.69	.31
2.1	0.88	3.1	2.9(9)	29(1)	.36(1)	290(10)	43.1(4)	.26(4)	127(15)	.65	.35
2.3	0.59	2.1	3.2(5)	26(1)	.35(1)	234(5)	40.1(2)	.24(2)	144(9)	.62	.38
2.5	0.43	1.8	3.1(3)	23(1)	.34(1)	197(3)	37.3(1)	.22(1)	159(6)	.58	.42
2.7	0.72	1.4	3.5(4)	21(1)	.35(1)	181(5)	35.4(2)	.20(2)	174(8)	.56	.44
3.1	0.57	1.4	3.1(3)	15.7(4)	.31(1)	163(4)	31.0(1)	.20(1)	196(6)	.45	.55
3.5	0.26	1.3	2.9(1)	11.6(2)	.2691	164(3)	27.4(1)	.19(1)	213(3)	.35	.65
3.9	0.36	1.0	2.9(1)	8.8(2)	.23(1)	163(6)	24.8(1)	.16(1)	223(3)	.27	.73
4.3	0.24	1.0	2.9(1)	6.8(1)	.25(1)	160(4)	22.5(1)	.15(1)	221(2)	.20	.80
4.7	0.48	1.5	2.9(1)	5.7(2)	.27(3)	158(10)	20.7(1)	.11(1)	219(3)	.16	.84
5.1	0.42	1.5	3.1(1)	5.1(2)	.28(1)	161(14)	19.1(1)	.09(1)	218(3)	.12	.88
5.7	0.47	1.9	3.1(1)	4.3(2)	.28(1)	170(27)	17.2(1)	.07(1)	205(3)	.08	.92
6.5	0.63	2.9	3.2(2)	2.9(3)	.33(17)	210(99)	15.1(1)	.04(1)	189(3)	.05	.95
a) $B_{DC} = 0.1\text{ T}$											
1.9	0.17	1.2	25.6(3)	33.8(3)	.30(1)	116(2)	50.8(1)	.16(1)	130(3)	.33	.67
2.1	0.19	1.0	23.9(2)	30.2(3)	.30(1)	99(3)	46.0(1)	.14(1)	134(3)	.29	.71
2.3	0.22	1.0	22.3(2)	27.4(3)	.31(2)	92(4)	42.5(1)	.13(1)	132(3)	.26	.74
2.5	0.29	1.5	21.2(3)	25.5(4)	.33(3)	80(5)	39.1(1)	.10(1)	136(3)	.24	.76
2.7	0.19	1.2	19.3(2)	22.6(2)	.30(2)	83(4)	36.2(1)	.12(1)	124(3)	.20	.80
3.1	0.24	0.94	17.2(2)	19.3(2)	.27(3)	94(6)	31.5(1)	.10(1)	122(3)	.14	.86
3.5	0.17	1.6	15.5(2)	16.7(1)	.23(4)	123(9)	27.9(1)	.10(1)	115(2)	.10	.90

$x_{LF} = (\chi_{T,LF} - \chi_S)/(\chi_T - \chi_S)$, $x_{HF} = (\chi_{T,HF} - \chi_{T,LF})/(\chi_T - \chi_S)$, $\chi_{T,HF} = \chi_T$, and $x_{HF} = 1 - x_{LF}$; χ in units of $10^6\text{ m}^3\text{ mol}^{-1}$.

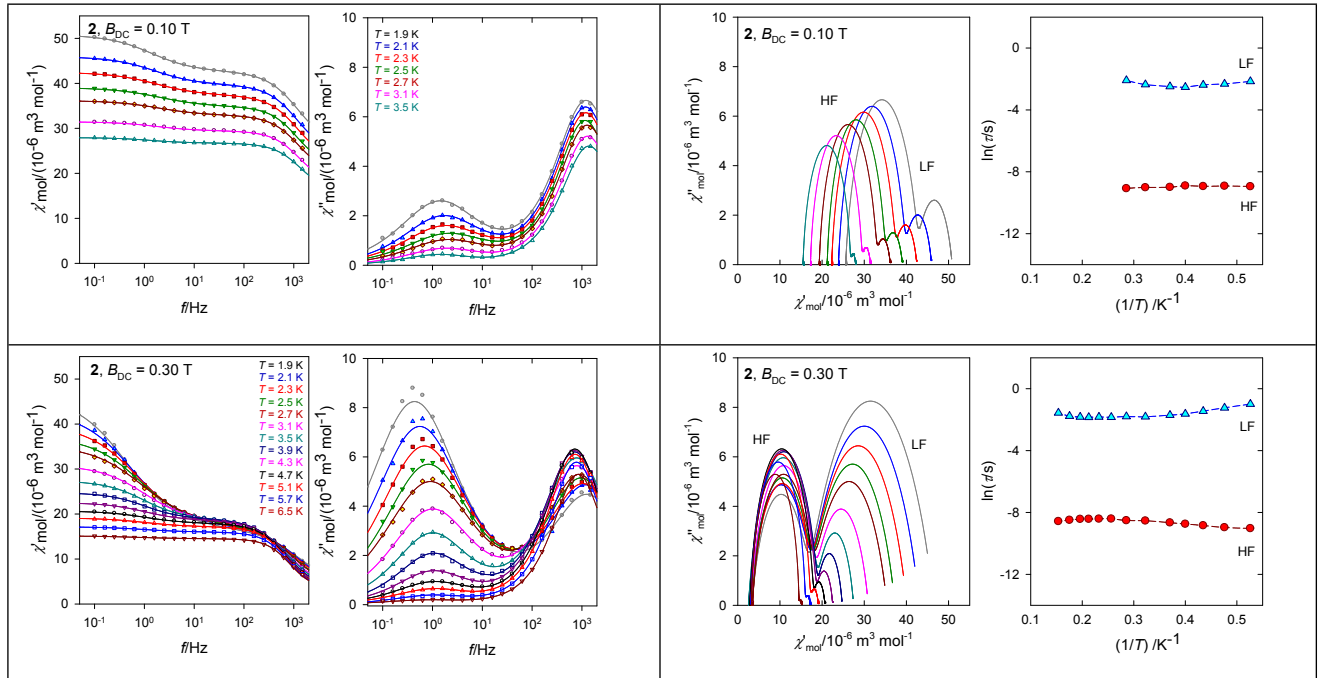
**Figure S8.** AC magnetic data for **2**. Solid lines – fitted by the extended two-set Debye model.

Table S5. Results of the fitting procedure for AC susceptibility components of **3** at $B_{DC} = 0.15$ T.

T/K	$R(\chi')$ /%	$R(\chi'')$ /%	χ_{LF}	α_{LF}	τ_{LF} / s	χ_{IF}	α_{IF}	τ_{IF} /10 ⁻³ s	χ_{HF}	α_{HF}	τ_{HF} /10 ⁻⁶ s	x_{LF}	x_{HF}
1.9	2.0	1.0	52(14)	.21(13)	1.29(23)	79(13)	.17(13)	74(21)	101(9)	.75(16)	964	.49	.23
2.3	1.7	1.3	29(8)	.01	0.77(9)	61(14)	.27(14)	72(25)	82(3)	.66(12)	999	.31	.28
2.7	1.6	2.0	24(16)	.01	0.50(8)	48(15)	.31(31)	58(51)	71(1)	.53(8)	965	.29	.35
3.1	2.5	2.3	22(10)	.03	0.36(10)	35(7)	.18	36(25)	62(1)	.40(6)	889(505)	.30	.48
3.5	2.1	1.5	16(9)	.06	0.34(14)	25(4)	.17	37(32)	55(1)	.34(4)	660(155)	.22	.60
3.9	1.1	.64	11(4)	.01	0.32(9)	18(1)	.16	39(22)	50(1)	.28(2)	450(30)	.14	.71
4.3	.63	.83	11(2)	.15(10)	0.29(8)	14(1)	.10	25(9)	46(1)	.21(1)	275(6)	.14	.78
4.7	.48	1.7	1.6(16)	.31(10)	0.18(7)	12(1)	.09	9.6(5)	42(1)	.13(1)	137(2)	.15	.81
5.1	.44	2.8	1.6(5)	.53(4)	0.09(1)	-	-	-	40(1)	.11(1)	64(1)	.16	.84
5.5	.67	3.8	9.1(8)	.56(9)	0.091(36)				37(1)	.14(4)	26(2)	.13	.87
5.9	.37	3.9	8.2(6)	.63(8)	0.097(4)				34(1)	.09(4)	12(1)	.11	.89
6.3	.35	8.1	8.7(33)	.80(18)	0.064				33(1)	.01	5.8(26)	.13	.87

$x_{LF} = (\chi_{T,LF} - \chi_S)/(\chi_T - \chi_S)$, $x_{IF} = (\chi_{T,IF} - \chi_{T,LF})/(\chi_T - \chi_S)$, $x_{HF} = (\chi_{T,HF} - \chi_{T,IF})/(\chi_T - \chi_S)$, $\chi_{T,HF} = \chi_T$, and $x_{IF} = 1 - x_{LF} - x_{HF}$. Fixed $\chi_S = 5.0 \times 10^{-6} \text{ m}^3 \text{ mol}^{-1}$; χ_i in units of $10^{-6} \text{ m}^3 \text{ mol}^{-1}$.

Ab initio calculation of the magnetic functions for 1.

Calculated energies of seven Kramers doublets:

Eigenvalues: cm-1 eV Boltzmann populations at T = 300.000 K

0:	0.00	0.0000	3.73e-01
1:	0.00	0.0000	3.73e-01
2:	299.43	0.0371	8.87e-02
3:	299.43	0.0371	8.87e-02
4:	474.36	0.0588	3.83e-02
5:	474.36	0.0588	3.83e-02
6:	2244.82	0.2783	7.87e-06
7:	2244.82	0.2783	7.87e-06
8:	2644.34	0.3279	1.16e-06
9:	2644.34	0.3279	1.16e-06
10:	2698.78	0.3346	8.92e-07
11:	2698.78	0.3346	8.92e-07
12:	2889.86	0.3583	3.57e-07
13:	2889.86	0.3583	3.57e-07